NANO LETTERS

2008
Vol. 8, No. 2
491−494

Isotope Effect on Band Gap and Radiative Transitions Properties of Boron Nitride Nanotubes

Wei-Qiang Han,*,† Hua-Gen Yu,‡ Chunyi Zhi,§ Jianbin Wang,§ Zhenxian Liu,|| Takashi Sekiguchi,§ and Yoshio Bando§

Center for Functional Nanomaterials, Department of Chemistry, Brookhaven National Laboratory, Upton, New York 11973, National Institute for Materials Science (NIMS), 1-1 Namiki, Tsukuba, Ibaraki 305-0044, Japan, Geophysical Laboratory, Carnegie Institution of Washington, 5251 Broad Branch Road, NW, Washington, District of Columbia 20015

Received October 10, 2007

ABSTRACT

We have carried out an isotope study on the band gap and radiative transition spectra of boron nitride nanotubes (BNNTs) using both experimental and theoretical approaches. The direct band gap of BNNTs was determined at 5.38 eV, independent of the nanotube size and isotope substitution, by cathodoluminescences (CL) spectra. At lower energies, several radiative transitions were observed, and an isotope effect was revealed. In particular, we confirmed that the rich CL spectra between 3.0 and 4.2 eV reflect a phonon–electron coupling mechanism, which is characterized by a radiative transition at 4.09 eV. The frequency red shift and peak broadening due to isotopic effect have been observed. Our Fourier transform infrared spectra and density functional theory calculations suggest that those radiative transitions in BNNTs could be generated by a replacement of some nitrogen atoms with oxygen.

Hexagonal boron nitride (h-BN) is a wide band gap semiconductor. Although its band structures have been extensively studied both experimentally and theoretically, they are not well understood. For example, the reported values of the direct band gap vary from 3.6 to 7.1 eV;[1−3] this divergence is due to the complicated electronic spectra caused by radiative transitions in BN. By analogy to carbon nanotubes, a boron nitride nanotube (BNNT) can be considered as a cylinder obtained when a single sheet of hexagonal BN is rolled onto itself. The electronic structures of BNNTs are very different from those of carbon nanotubes because of the wide gap of the BN sheets compared to the zero gap in graphite.[4] In contrast to carbon nanotubes, whose electric properties depend on the chirality and diameter of the nanotubes, theoretical values of the direct band gap of BNNTs with a diameters more than 9.5 Å (a value about that of a (12, 0) nanotube) are about equal to that of h-BN (around 5.5 eV) and nearly independent of the nanotube's diameter, chirality, and wall−wall interactions.[5−8]

Only a few experimental studies of band gap structures of BNNTs have been reported and often the results are contradictory. Lauret et al. directly measured the optical properties of single-walled BN nanotubes (mixed with boric acid, boron, silica, and other BN structures) using a UV−vis-NIR spectrophotometer and observed three absorption peaks at 4.45, 5.5, and 6.15 eV.[9] They proposed that the first two transitions could result from a quantification issue due to the rolling up of h-BN sheet. Arenal et al. carried out electron energy loss-spectroscopy (EELS) measurements on the optical gaps of single-walled and multiwalled BNNTs. They found that the optical gap measured at 5.8 ± 0.2 eV is independent of the nanotubes' geometry.[10] Czerw et al. undertook a STM/STS investigation of multiwalled BNNTs with diameters above 5 nm. Their results revealed bandgaps at 4.5 and 4.8 eV that had no correlation to nanotube's diameter or chirality.[11] Ishigami et al. studied double-walled BNNTs with diameters of 2.7 ± 0.3 nm and found one nanotube has a band gap of 3.8 eV under an applied electric field of 0.08 V/Å.[12] Further, Wu et al. observed the strong photoluminescence (PL) of a wide emission peak around 3.9 eV in their Raman and time-resolved photoluminescence spectroscopic studies of multiwalled BNNTs at room temperature.[13] Phonon replica features were found for BN and $B_xC_yN_z$ nanotubes. Owing to the limitation of the excitation wavelength of the used laser (244 nm), the PL spectra could only reveal luminescence peaks whose energies are less than 5 eV.[13] Cathodoluminescences (CL) of BNNTs were studied by Zhi et al. who noted a strong luminescence peak located

* Corresponding author. E-mail: whan@bnl.gov.
† Center for Functional Nanomaterials, Brookhaven National Laboratory.
‡ Department of Chemistry, Brookhaven National Laboratory.
§ National Institute for Materials Science.
|| Carnegie Institution of Washington.

10.1021/nl0726151 CCC: $40.75
Published on Web 01/04/2008

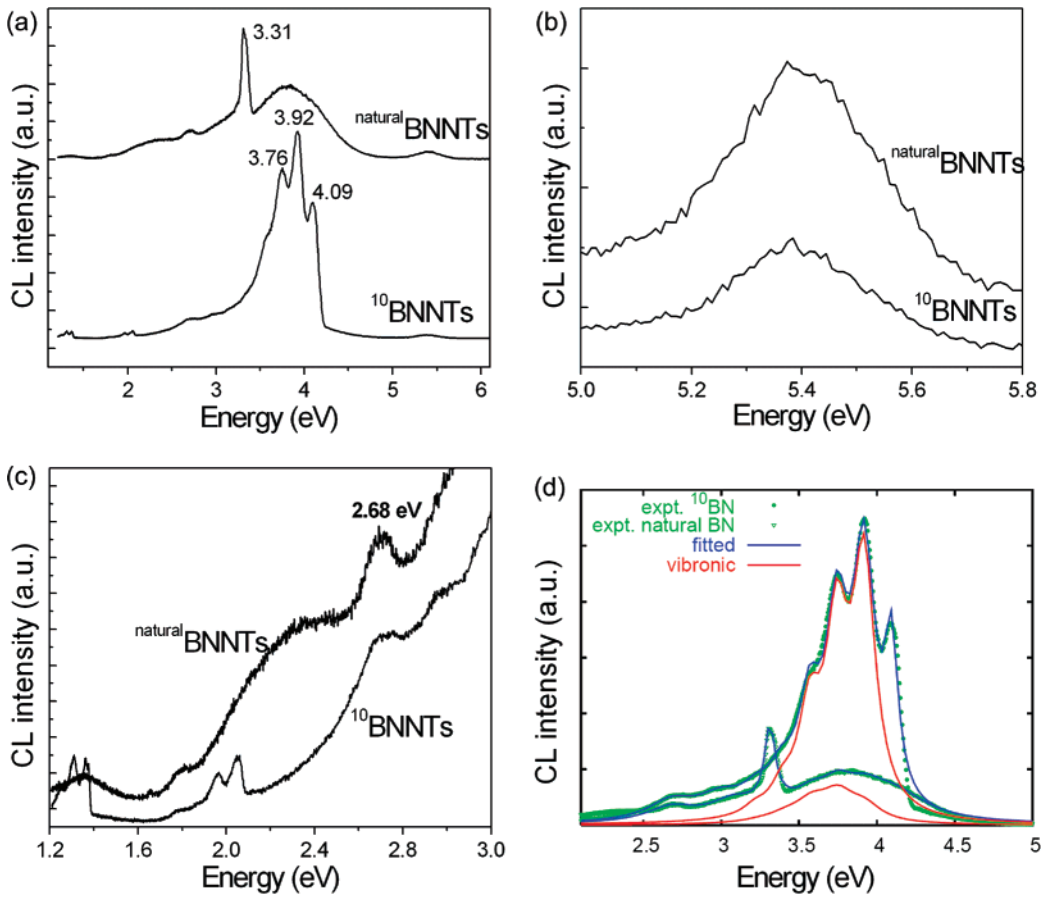

Figure 1. (a) CL spectra taken from thick natural BN and ^{10}BN nanotubes; (b) an enlarged image in the range 5.0−5. 8 eV; (c) an enlarged image in the range 1.2−3.2 eV; and (d) a comparison of fitted spectra with experimental ones for the ^{10}BN and natural BN NTs, where the red curves refer to the vibronic spectra with a phonon replica of $n = 1\sim5$.

around 3.3 eV and a weak peak at 4.1 eV.[14] In particular, those previous investigations were obtained from natural BNNTs that consist of 20% ^{10}B and 80% ^{11}B.[15]

Because most physical properties of BNNTs are based on the value of band gap, it is highly desirable to precisely determine them experimentally. We note that the measurement can be remarkably affected by the quality of the source of samples (such as size distribution, nanotubes percentages, and impurities), as well as by the methods used for characterization. In this work, we studied in detail both the band structures and the radiative transitions of different sized BN nanotubes using CL spectroscopy and B isotope techniques. A CL spectrum is yielded from light emissions from a crystal via the radiative recombination of electrons and holes. Here, radiative recombination centers are associated with their characteristic luminescence. Nonradiative recombination centers in direct gap semiconductors are also detected as the decrease intrinsic luminescence.[16,17]

The BNNTs used here were prepared by a metal-assisted chemical synthetic route in which the B atoms reacted with a mixture of MgO and SnO under ammonia atmosphere to form multiwalled BN nanotubes.[18,19] The as-generated products were treated at 1600 °C under vacuum to remove any possible remnants of impurity. The final purity of the nanotubes was about 90%; the rest consisted of BN fullerene-like nanoparticles. The wall numbers and tube diameters were typically tens and 20−120 nm, respectively. We called them thick BNNTs. ^{10}BNNTs were made under the same experimental conditions except that ^{10}B powders (Cambridge Isotope Lab. Inc., ^{10}B, 92−99%) were used rather than the natural B powders. A field-emission scanning electron microscope equipped with a CL system was used for the luminescence characterization.[17]

Figure 1a shows the CL spectra taken from a bunch of natural BN and ^{10}BN nanotubes, respectively. In the CL spectrum of ^{10}BN NTs, along with the direct band gap at 5.38 eV (Figure 1b shows the detail), a rich structure spanning from 3.0 to 4.2 eV was observed. It arises from a radiative transition at $E_0 = 4.092$ eV and its coupling with a phonon mode of the BN nanotube. The equal spacing peaks at lower energies can be assigned to the recombination of multiphonon and electron emissions according to an energy and momentum conservation law. A spectrum analysis within 2.4−5.0 eV is displayed in Figure 1d. The fitted spectra are simulated by summing over nine individual Lorentzian lineshape $[G(E;E_0,\Gamma) = 1/\pi\ \Gamma/((E - E_0)^2 + \Gamma^2)]$ terms;[20] among them, those four peaks at 4.092, 3.313, 3.081, and 2.679 eV are identified as electronic transitions (i.e., called radiative transitions here). The red curves represent the spectra contributed from only those electron emissions induced by phonons, which clearly shows a progression up to five phonon replicas. For these five transitions, the peak energies

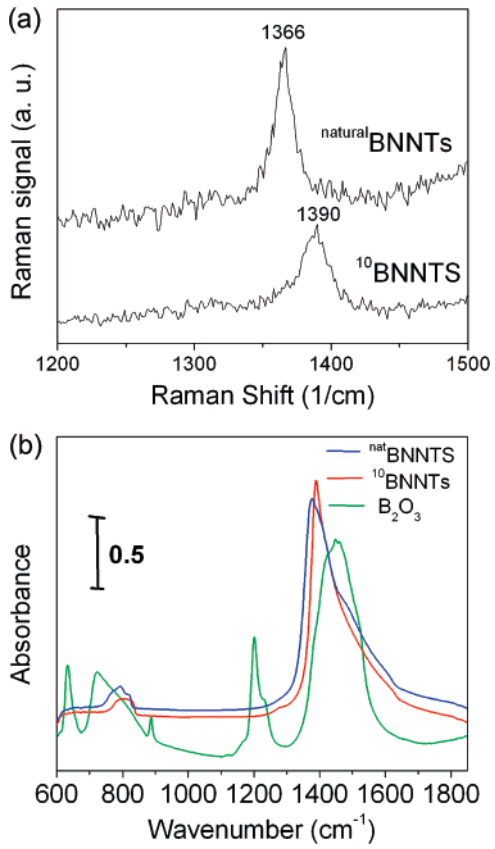

Figure 2. (a) Raman spectra taken from thick ^{10}BNNTs and natural BNNTs. The peak positions of the zone-center, counter-phase B−N vibration mode (E_{2g}) within BN sheets for ^{10}BNNTs and natural BNNTs are at 1390 cm^{-1} and 1366 cm^{-1}, respectively. (b) FTIR spectra taken from thick ^{10}BNNTs, natural BNNTs, and B_2O_3 powders.

are defined by equal spacing energies $E_n = E_0 - n\nu$ with a common width Γ_n and $n = 1-5$, where ν is the phonon frequency. For the ^{10}BN NTs, we extracted a phonon frequency of 0.1752 eV (or 1413 cm^{-1}) with a full width at the half-maximum (FWHM) of 0.087 eV. This value agrees well with our experimental data of 1390 cm^{-1} determined from the strong peak of the Raman spectra (Figure 2a) of the ^{10}BNNTs; it is assigned to a B−N bond stretching deformation mode. The discrepancy between these values falls within the fitted error bars.

Because the bandgaps depend only on the electronic structure of BNNTs, the same vibronic coupling effect was observed in the CL spectrum of natural BNNTs at the same energy region (3.0−4.2 eV), although the resolution was lower. However, the electronic properties of BNNTs are independent of the nanotube's size and chirality, which allows us to correspondingly analyze the spectrum for the natural BNNTs by fixing the four electronic bands at the same values as in the ^{10}BNNTs. Similarly, a replica structure up to five phonons has been observed as shown in Figure 1a,d. The determined frequency and the FWHM are 1381 cm^{-1} and 0.130 eV, respectively. Compared to those for the ^{10}BNNTs, the frequency exhibits a red shift of 32 cm^{-1} whereas its width significantly increases. The red shift is consistent with our Raman measurement (24 cm^{-1}) and is due to the isotopic effect of B. Natural BNNTs consist of 20% ^{10}B and 80% ^{11}B and thus include more heavy B atoms than ^{10}BNNTs. Such an effect also induces line broadening as frequencies for all vibrational modes in natural BNNTs are statistically determined by averaging all the existing ensembles of ^{10}B and ^{11}B distributions in tubes. As a result, for each mode it has more broadened distribution than that of BNNTs without involving isotopes. Therefore, the isotopic effect that causes such broadened phonon−electron transition bands entails a dramatic decrease in the resolution of the related spectrum. Interestingly, the frequency red shift and peak broadening due to isotopic effect have recently been observed for single-walled carbon nanotubes and multiwalled carbon nanotubes.[21−23]

In particular, we have employed the same physical model to closely fit the spectra of both ^{10}BNNTs and natural BNNTs. This concretely confirms that the phonon−electron coupling mechanism adopted here is correct. Furthermore, a strong peak at 3.313 eV is apparent for the natural BNNTs. Its relative intensity compared to the band at 4.092 eV is 2.51. In contrast, for the ^{10}BNNTs the transition at 3.313 eV is too weak to be noticed. According to our simulations, the corresponding relative intensity is only 0.12, that is, about 21 times weaker than that in ^{10}BNNTs. Nevertheless, this band does exist in ^{10}BNNTs although we still do not know what causes such a faint emission. One possible explanation is the contamination of oxygen species in the tubes.

The radiative transitions in the BN tubes were induced by defects or impurities in the nanotubes. One possible mechanism is that oxygen atoms partially substitute some B and/or N atoms in the BNNTs during their synthesis and treatments. To investigate the likelihood, we compared the FTIR spectra of the BNNTs with that of B_2O_3 powder, as shown in Figure 2b. The major peak positions for the ^{10}BN and natural BNNTs, respectively, are at 1392[1] and 1376 cm^{-1} (also revealed by the Raman spectra), which are assigned to a B−N stretching deformation vibration mode. The obvious overlap of both peaks with a small peak can be assigned to B−O stretching mode (1460 cm^{-1}). Similar features are also observed for the spectra peaked at 800 cm^{-1}. These data indicate the existence of some B−O bonds in our BN nanotubes. In other words, O atoms have partially substituted N or B atoms in the B−N networks. Besides the B−O stretching mode, B−O deformation modes at 1196, 884, and 634 cm^{-1} are also seen in the spectrum from the B_2O_3 reference power.[24] Nevertheless, while these peaks occur in the spectra of both ^{10}BN and natural BN nanotubes they are weakened or diminished due to the nanotubes' two-dimensional structure.

In addition, we also undertook a theoretical study of an O atom-replaced BNNT using a BLYP (a combination of Becke's exchange functional with Lee, Yang, and Parr's nonlocal correlation functional)[25,26] density functional theory (DFT) method with periodic boundary conditions. An O-substituted BN (5, 5) nanotube was used as a model. The Martins−Troullier (MT)[27] pseudopotentials represented the core electrons in each atom, while a plane wave basis set was employed for the valance electrons with a cut off energy of 80 Ry. In the calculations, a 5 × 1 × 1 supercell consisting

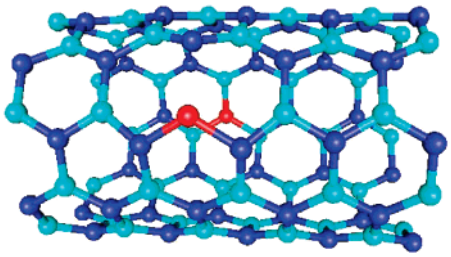

Figure 3. Structure of an oxygen atom-substituted BN (5,5) tube calculated with a BLYP DFT method, where B, N, and O atoms are shown in sky blue, deep blue and red, respectively.

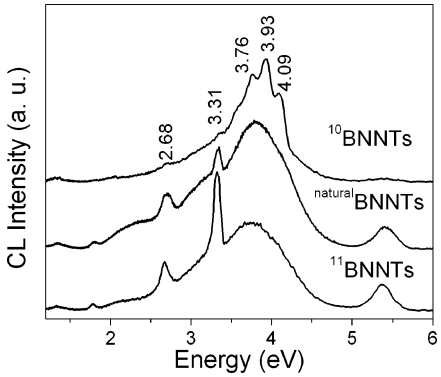

Figure 4. CL spectra taken from thin ^{10}BNNTs, ^{11}BNNTs, and natural BN nanotubes.

of 100 atoms (49 B, 49 N, and 2 O atoms) was simulated with two k-points in the *x* direction and only one Γ-point in either the *y* or *z* direction, where the nanotube was placed along the *x*-axis. The final optimized cell size in Å is 12.5899 × 15.0 × 15.0 so that the nanotube wall-to-wall distance is about 8.0 Å, i.e, large enough to minimize the effect from adjacent tubes. All electronic structure calculations were done using the Car−Parrinello molecular dynamics (CPMD) program.[28] Figure 3 shows the optimized structure. We found that when B is replaced with O, one N−O bond is broken, creating a defect on the tube. On the other hand, the replacement of N with O still maintains the same connectivity as the original BN (5, 5) tube. Therefore, this theoretical study confirms that BN_xO_{1-x} tubes are stable, solidly supporting our experimental observations.

For comparison, we used a carbon nanotube-substitution reaction[29,30] to prepare thin multiwalled BNNTs (single-walled BNNTs are also found occasionally), whose typical wall numbers and diameters are 2−7 layers and 3−9 nm, respectively. We call them thin BNNTs. The percentage of nanotubes is about 70% with 30% mainly BN fullerene-like nanoparticles and some BN nanosheets. For synthesizing isotope ^{10}BN and ^{11}BN nanotubes, natural B_2O_3 was replaced by $^{10}B_2O_3$ (Euriso-top, $^{10}B_2O_3$, 96.50% atom ^{10}B) and $^{11}B_2O_3$ (Euriso-top, $^{11}B_2O_3$, 99.98% atom ^{11}B), respectively.[19] Figure 4 shows the CL spectra of thin ^{10}BN, ^{11}BN, and natural BN nanotubes; they give the same results as in Figure 1 for thick BNNTs. As expected, the direct band gap at 5.38 eV is independent of the nanotubes' size. This value is slightly smaller than the theoretical prediction of 5.5 eV and the EELS result of 5.8 ± 0.2 eV but apparently larger than the STM/STS measurement of 4.6 eV. We also noticed the radiative transitions originating from the substitution of the O atom for N or defects in BN networks as discussed above.

Recently, Watanabe et al. showed that single crystalline h-BN has a direct band gap of 5.765 eV (215 nm), which was confirmed by the accelerated electron excitation experiments that demonstrated an ultraviolet lasing at 215 nm at room temperature.[3] This finding implies the potential application of hexagonal BN for compact ultraviolet laser devices with larger band gap than that of GaN (3.4 eV). Therefore, this band gap and radiative transitions study is expected very helpful for developing prospective novel optical and electric nanodevices based on BNNTs.

Acknowledgment. This work is supported by the U.S. DOE under Contract DE-AC02-98CH10886 through Laboratory Directed Research and Development Fund of Brookhaven National Laboratory (to W.H.) and by a fund from ICYS at NIMS for W.H.

References

(1) Zupan, J.; Kolar, D. *J. Phys. C* **1972**, *5*, 3097.
(2) Hoffman, D. M.; Doll, G. L.; Eklund, P. C. *Phy. Rev. B* **1984**, *30*, 6051.
(3) Watanabe, K.; Taniguchi, T.; Kanda, H. *Nat. Mater*. **2004**, *3*, 404.
(4) Chopra, N. G.; Luyken, R. J.; Cherrey, K.; Crespi, V. H.; Cohen, M. L.; Louie, S. G.; Zettl, A. *Science* **1995**, *269*, 966.
(5) Rubio, A.; Corkill, J.; Cohen, M. L. *Phys. Rev. B* **1994**, *49*, 5081.
(6) Blasé, X.; Rubio, A.; Louie, S. G.; Cohen, M. L. *Europhys. Lett.* **1994**, *28*, 335.
(7) Park, C. H.; Spataru, C. D.; Louie, S. G. *Phy. Rev. Lett.* **2006**, *96*, 126105.
(8) Wirtz, L.; Marini, A.; Rubio, A. *Phy. Rev. Lett.* **2006**, *96*, 126104.
(9) Lauret, J. S.; Arenal, R.; Ducastelle, F.; Loiseau, A. *Phy. Rev. Lett.* **2005**, *94*, 037405.
(10) Arenal, R.; Stephan, O.; Kociak, M.; Taverna, D.; Loiseau, A.; Colliex, C. *Phys. Rev. Lett.* **2005**, *95*, 127601.
(11) Czerw, R.; Webster, S.; Carroll, D. L.; Vieira, S. M. C.; Birkett, P. R.; Rego, C. A.; Roth, S. *Appl. Phys. Lett.* **2003**, *83*, 1617.
(12) Ishigami, M.; Sau, J. D.; Aloni, S.; Cohen, M. L.; Zettl, A. *Phy. Rev. Lett.* **2005**, *94*, 056804.
(13) Wu, J.; Han, W. Q.; Walukiewicz, W.; Ager, J. W.; Shan, W.; Haller, E. E.; Zettl, A. *Nano Lett*. **2004**, *4*, 647.
(14) Zhi, C.; Bando, Y.; Tang, C.; Golberg, D.; Xie, R.; Sekigushi, T. *Appl. Phys. Lett.* **2005**, *86*, 213100.
(15) Han, W. Q.; Todd, P. J.; Strongin, M. *Appl. Phys. Lett.* **2006**, *89*, 173103.
(16) Yacobi, B. G.; Holt, D. B. *Cathodoluminescence Microscopy of Inorganic Solids*; Plenum: New York, 1990.
(17) Sekiguchi, T.; Sumino, K. *Rev. Sci. Instrum.* **1995**, *66*, 4277.
(18) Tang, C.; Bando, Y.; Sato, T.; Kurashima, K. *Chem. Commun.* **2002**, 1290.
(19) Zhi, C.; Bando, Y.; Tang, C.; Golberg, D. *Solid State Commun.* **2005**, *135*, 67.
(20) Tipping, R. H.; Ma, Q.; Boulet, C. *AIP Conf. Proc.* **2006**, *874*, 338.
(21) Simon, F.; Kramerger, C.; Pfeiffer, R.; Kuzmany, H.; Zolyomi, V.; Kurti, J.; Singer, P. M.; Alloul, H. *Phys. Rev. Lett.* **2005**, *95*, 017401.
(22) Miyauchi, Y.; Maruyama, S. *Phys. Rev. B* **2006**, *74*, 035415.
(23) Zolyomi, V.; Simon, F.; Rusznyak, A.; Pfeiffer, R.; Peterlik, H.; Kuzmany, H.; Kurti, J. *Phy. Rev. B* **2007**, *75*, 195419.
(24) Moon, O. M.; Kang, B. C.; Lee, S. B.; Boo, J. H. *Thin Solid Films* **2004**, *464-465*, 164.
(25) Becke, A. D. *Phys. Rev. A* **1998**, *38*, 3098.
(26) Lee, C.; Yang, W.; Parr, R. G. *Phys. Rev. B* **1988**, *37*, 785.
(27) Troullier, N.; Martins, J. L. *Phys. Rev. B* **1991**, *43*, 8861.
(28) CPMD, version. http://www.cpmd.org/ (accessed).
(29) Han, W. Q.; Bando, Y.; Kurashima, K.; Sato, T. *Appl. Phys. Lett.* **1998**, *73*, 3085.
(30) Han, W. Q.; Mickelson, W.; Cumings, J.; Zettl, A. *Appl. Phys. Lett.* **2002**, *81*, 1110.

NL0726151